4-2014

Glutamate transporter control of ambient glutamate levels

Weinan Sun

Denis M. Shchepakin

Leonid Kalachev

Michael P. Kavanaugh

Neurochemistry International 73 (2014) 146–151

Contents lists available at ScienceDirect

Neurochemistry International

journal homepage: www.elsevier.com/locate/nci

Glutamate transporter control of ambient glutamate levels

Weinan Sun [a], Denis Shchepakin [b], Leonid V. Kalachev [a,b], Michael P. Kavanaugh [a,*]

[a] Center for Structural and Functional Neuroscience, The University of Montana, Missoula, MT 59812, United States
[b] Department of Mathematics, The University of Montana, Missoula, MT 59812, United States

ARTICLE INFO

Article history:
Available online 22 April 2014

Keywords:
Glutamate transport
Ambient neurotransmitter
Tonic signaling
Microdialysis

ABSTRACT

Accurate knowledge of the ambient extracellular glutamate concentration in brain is required for understanding its potential impacts on tonic and phasic receptor signaling. Estimates of ambient glutamate based on microdialysis measurements are generally in the range of ~2–10 μM, approximately 100-fold higher than estimates based on electrophysiological measurements of tonic NMDA receptor activity (~25–90 nM). The latter estimates are closer to the low nanomolar estimated thermodynamic limit of glutamate transporters. The reasons for this discrepancy are not known, but it has been suggested that microdialysis measurements could overestimate ambient extracellular glutamate because of reduced glutamate transporter activity in a region of metabolically impaired neuropil adjacent to the dialysis probe. We explored this issue by measuring diffusion gradients created by varying membrane densities of glutamate transporters expressed in *Xenopus* oocytes. With free diffusion from a pseudo-infinite 10 μM glutamate source, the surface concentration of glutamate depended on transporter density and was reduced over 2 orders of magnitude by transporters expressed at membrane densities similar to those previously reported in hippocampus. We created a diffusion model to simulate the effect of transport impairment on microdialysis measurements with boundary conditions corresponding to a 100 μm radius probe. A gradient of metabolic disruption in a thin (~100 μm) region of neuropil adjacent to the probe increased predicted [Glu] in the dialysate over 100-fold. The results provide support for electrophysiological estimates of submicromolar ambient extracellular [Glu] in brain and provide a possible explanation for the higher values reported using microdialysis approaches.

1. Introduction

During synaptic transmission, glutamate transporters restrict the spatiotemporal pattern of ionotropic and metabotropic glutamate receptor signaling (for review see Tzingounis and Wadiche, 2007). In addition to their roles in shaping the dynamics of synaptically released glutamate, glutamate transporters also help maintain low steady-state glutamate levels. Given the stoichiometry of ion coupling to glutamate uptake, the theoretical lower limit of extracellular glutamate in brain is approximately 2 nM (Zerangue and Kavanaugh, 1996; Levy et al., 1998). Many studies using intracerebral microdialysis have reported levels of ambient glutamate ⩾ 2 μM, three orders of magnitude higher than the theoretical lower limit (Benveniste et al., 1984; Lerma et al., 1986; for reviews see Cavelier et al., 2005; Nyitrai et al., 2006). By contrast, reports of ambient glutamate concentration estimated from electrophysiological measurement of tonic NMDA receptor activity in hippocampal slice range from 87 to 89 nM (Cavelier and Attwell, 2005; Le Meur et al., 2007) to as low as 25 nM (Herman and Jahr, 2007).

Accurate knowledge of the ambient glutamate concentration in different brain regions is important for evaluating its effects on synaptic transmission. Several ionotropic and metabotropic glutamate receptor subtypes are activated by low micromolar concentrations of glutamate, and tonic exposure in this range profoundly inhibits synaptic circuitry *in vitro* (Zorumski et al., 1996). Glutamate transporters play a dominant role in limiting ambient glutamate, as pharmacological inhibition of transport has been shown to lead to a rapid increase in ambient glutamate causing increased tonic NMDA receptor signaling (Jabaudon et al., 1999; Cavelier and Attwell, 2005; Le Meur et al., 2007; Herman and Jahr, 2007).

In this work we attempt to integrate data in the literature with new *in vitro* measurements and *in vivo* modeling of diffusion gradients formed by glutamate transporters. Proceeding from the assumption that in steady-state conditions, the volume-averaged rates of release and uptake of glutamate are equal, we show the

* Corresponding author. Tel.: +1 4062434398; fax: +1 4062434888.
E-mail address: michael.kavanaugh@umontana.edu (M.P. Kavanaugh).

http://dx.doi.org/10.1016/j.neuint.2014.04.007
0197-0186/

influence of glutamate transporter membrane density on steady-state diffusion gradients in a density range relevant to *in vivo* brain expression. We suggest that metabolic impairment of glutamate transport in a shallow boundary region of a microdialysis probe can account for the discrepancies between estimates of ambient glutamate from dialysis and electrophysiological approaches.

2. Materials and methods

2.1. Xenopus oocyte recording

Approximately 50 ng of human EAAT3 cRNA was microinjected into stage V–VI Xenopus oocytes and recordings were made 1–6 d later. Recording solution contained 96 mM NaCl, 2 mM KCl, 1 mM $MgCl_2$, 1.8 mM $CaCl_2$, and 5 mM Hepes (pH 7.5). Microelectrodes were pulled to resistances between 1 and 3 MΩ and filled with 3 M KCl. Data were recorded with Molecular Devices amplifiers and analog–digital converters interfaced to Macintosh computers. Data were analyzed offline with Axograph X (v.1.0.8) and KaleidaGraph (v 3.6; Synergy) software. For stopped flow measurements, oocytes were voltage clamped at −60 mV in a perspex recording chamber in which glutamate depletion in the absence of perfusion was <1% of the total in the recording chamber. Transporter surface density was estimated from current measurements assuming a coupled current of 2 charges/cycle at E_{Cl} (−20 mV), turnover rate of 15/s, oocyte surface area 2.85×10^7 μm^2, and transport voltage-dependance of e-fold/76 mV (Wadiche et al., 1995; Zerangue and Kavanaugh, 1996). Current amplitudes were fitted to the Michaelis–Menten relationship:

$$I_{[Glu]} = I_{max}[Glu]/\{K_M + [Glu]\}$$

2.2. Mathematical modeling of [Glu] profile near the microdialysis probe

Our microdialysis probe model can be described by the following diffusion equation in polar coordinates with sink and source in the right hand side:

$$\partial u/\partial t = D \cdot \ (1/r) \cdot \ \partial/\partial r \ [r \cdot \partial u/\partial r] - J \cdot \ u/(K_m + u) + K_L$$

where u corresponds to L-glutamate concentration. The first term in the right hand side is a Laplace operator in polar coordinates multiplied by a diffusion coefficient D. The second term represents the Michaelis–Menten transport sink in the tissue, and the third term K_L represents the leak, which is treated as a constant. The parameter J is a function of distance r from the probe center, and describes the spatial dependence of transporter impairment between the healthy and damaged tissue. The spatial metabolic damage near the probe is approximated as a Gaussian curve, and we define the function J as:

$$J(r) = 0 \text{ when } 0 \le r \le L$$

$$J(r) = J_{max} \cdot 1 - e\text{^}[-(r-L)2/2 \cdot \ sigma^2] \text{ when } r > L$$

where L is the radial boundary for the microdialysis probe and sigma represents the distance from the probe boundary characterizing the Gaussian damage function. The boundary conditions for the model are:

$$\partial u/\partial r|_{r=0} = 0$$

$$u(t, \infty) = u_s$$

The initial condition is

$$u(t, r) = u^* \text{ when } 0 \le r \le L$$

$$u(t, r) = u_s \text{ when } r > L$$

This model cannot be solved analytically because of the nonlinear term in the right hand side of the equation, so it was solved numerically by space discretization, which transforms it into system of ordinary differential equations. The leak rate constant (K_L) is related to ambient [Glu], volumetric glutamate transporter concentration [GluT] (140 μM, Lehre and Danbolt, 1998), transporter K_M value, and maximal turnover rate J_{max} by the equation:

$$K_L = [Glu]_{ambient}/(K_m + [Glu]_{ambient}) \cdot [GluT] \cdot J_{max}$$

3. Results

3.1. Diffusive concentration gradients formed by glutamate transporters

Co-expression studies of NMDA receptors with transporters for its co-agonists glycine and glutamate have shown that transporters can limit receptor activity by establishing diffusion-limited transmitter concentration gradients (Supplisson and Bergman, 1997; Zuo and Fang, 2005). We studied the concentration gradients formed by passive diffusion from a pseudo-infinite glutamate source in a perspex chamber to the glutamate sink established by transporters on the cell surface. Oocytes expressing the human neuronal glutamate transporter EAAT3 were voltage-clamped at −60 mV and superfused with varying concentrations of glutamate at a linear flow rate of 20 mm/s flow followed by a stopped-flow interval (Fig. 1). Steady-state currents elicited by glutamate perfusion relaxed to a lower steady-state level when flow was stopped, and following resumption of flow, currents rapidly recovered to initial values. The reduction in current amplitude during zero flow conditions was likely due to the formation of a diffusion-limited concentration gradient resulting in reduced surface [Glu], because the ratio of the current amplitudes with and without flow were dependent on the concentration of glutamate in the perfusate, and in all cases the amount of glutamate transported was <1% of the total glutamate in the chamber (i.e. a pseudo-infinite glutamate source; Fig. 1B–D). This gradient was also reflected in a significant shift in the concentration-dependance of steady-state currents in flow and stopped-flow conditions (K_M value for L-glutamate of 32 ± 2 and 216 ± 37 μM, respectively, $n = 4$; $p < 0.002$), while the I_{max} values were not significantly different.

3.2. Transporter density influence on kinetic parameters

Glutamate transporters are expressed at different densities among structures in the CNS, and transporter density and/or kinetics can be altered in different pathological circumstances such as trauma and ischemia. Because steady-state ambient [Glu] reflects a homeostatic balance of uptake and leak sources, changes in transport may result in significantly different steady state glutamate levels. We tested the influence of the surface density of glutamate transporters on the concentration gradient formed by passive glutamate diffusion during stopped-flow experiments by monitoring currents induced by 10 μM glutamate. With increasing transporter expression levels, the steepness of the concentration gradient formed during stopped-flow conditions was increased, as reflected in the changing ratio of the steady-state currents in flow and stopped-flow conditions (Fig. 2A and B).

Even with continuous flow, evidence for formation of a concentration gradient between the cell surface and bulk solution was observed. Oocyte membranes have a microvillar structure that can act as tortuous diffusion barrier (see Supplisson and Bergman, 1997). In a group of 29 oocytes with varying expression levels, steady-state K_M values measured with chamber flow

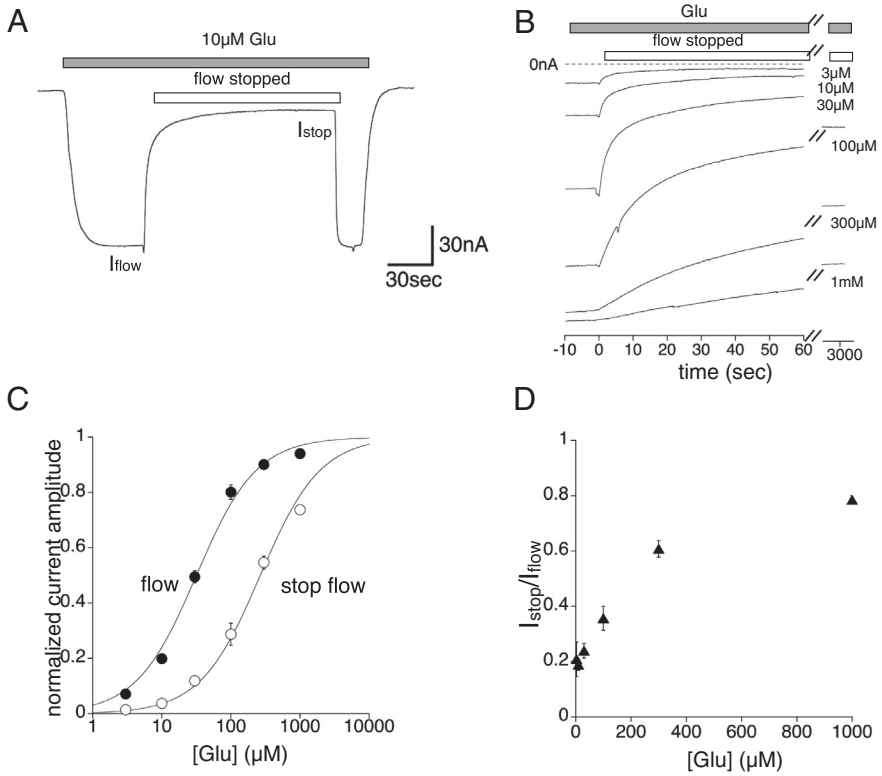

Fig. 1. Glutamate transport acts as a sink to form a concentration gradient between the extracellular volume and the membrane surface. (A) Current induced by 10 μM glutamate decays to a lower steady state flow under stopped-flow conditions at −60 mV. (B) Current responses to varying [Glu] with and without flow at −60 mV. (C) Glutamate concentration-dependance of steady-state currents in flow and stopped-flow conditions. (km value with flow: 32 ± 2 μM; stopped-flow: 215 ± 37 μM; $n = 4$, $p = 0.0014$). (D) Glutamate concentration-dependance of the ratio of current amplitudes in stopped-flow and flow conditions.

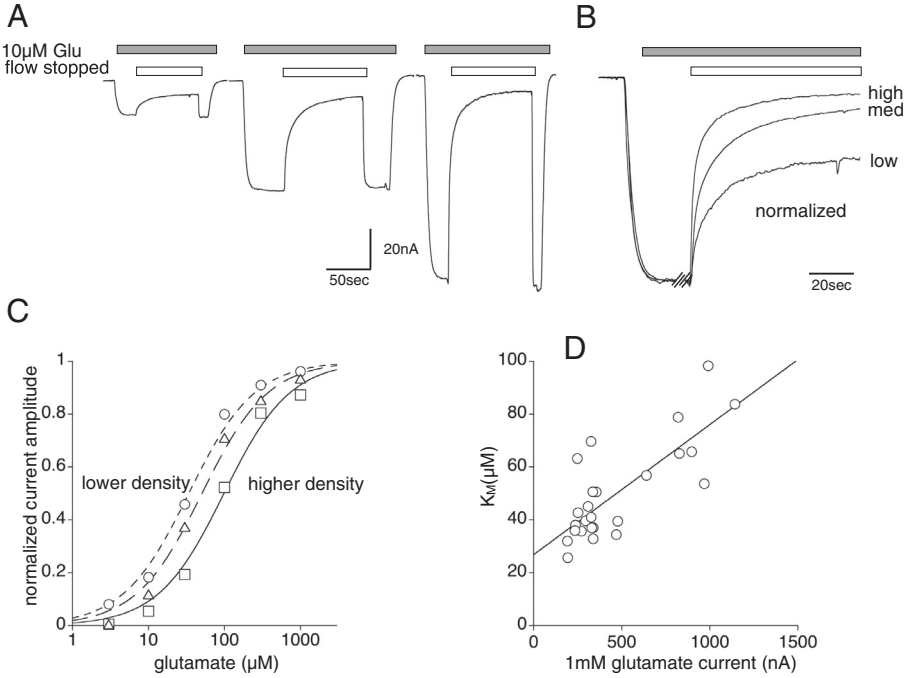

Fig. 2. Glutamate concentration gradients are a function of transporter density. (A) Representative traces of stopped-flow experiments with oocytes expressing different transporter densities. (B) Currents from cells in (A) normalized to the steady state current. (C) Glutamate concentration-dependance of steady-state currents with low, medium and high expression levels. (km values: low expression: 33 μM, medium expression: 50 μM and high expression: 98 μM. Transport current amplitudes (1 mM glutamate) are 260, 332 and 688 nA, respectively). (D), K_M values from 29 oocytes with different expression levels (fitted with linear regression, $r = 0.78$; y intercept = 26.8 μM).

(20 mm/s) increased approximately 4-fold as transporter current induced by 1 mM glutamate increased from ~200 to ~1100 nA (Fig. 2C and D). Thus, there is an effect of the concentration gradient formed by transporters even with continuous flow, resulting in a discrepancy between the measured and actual glutamate K_M value. We extrapolated a linear function relating the measured K_M value to the transport current density (Barry and Diamond, 1984), yielding an estimate of the intrinsic K_M value of approximately 27 μM ($r = 0.78$; Fig. 2D).

3.3. Surface [Glu] as a function of transporter density

While the dependance of steady-state K_M on transporter density reflects the fact that the true glutamate concentration at the cell surface is reduced by uptake, the concentration difference associated with the diffusion gradient is minimal at when high concentrations of glutamate are applied by continuous flow. In oocytes expressing varying densities of transporters, we recorded currents induced by superfusion of 1 mM glutamate in order to generate the theoretically predicted current amplitude in each cell as a function of [Glu] from the Michaelis–Menten function using the intrinsic K_M value of 27 μM (Fig. 3A). We then recorded the actual steady-state current amplitude in each cell in response to 10 μM glutamate under stopped-flow conditions and compared these to the values predicted by the Michaelis–Menten function. There was a discrepancy between the theoretically predicted and measured values, and this difference increased monotonically with transporter density. We inferred the actual glutamate surface concentration in the stopped-flow condition with 10 μM glutamate in the chamber from the measured current amplitudes using the uniquely determined Michaelis–Menten function for each cell (Fig. 3A and inset). The inferred surface concentration was then plotted as a function of transporter density. There was a supralinear effect of transporter density on surface [Glu] in stopped-flow conditions (Fig. 3B). Transporter density in this group of cells ranged from 234 to 5165 transporters per μm^2. At low expression levels, the estimated [Glu] approached the 10 μM source concentration. However, at transporter densities of ~5000 μm^{-2} (compare with estimates in hippocampus of 10,800 μm^{-2}; Lehre and Danbolt, 1998), surface [Glu] was estimated to be reduced to ~50 nM, roughly 200-fold lower.

3.4. Modeling the glutamate concentration profile near a microdialysis probe

We constructed a diffusion model to simulate the spatial profile of glutamate near a microdialysis probe (see Section 2). From quantitative immunoblotting, the glutamate transporter density in hippocampus has been estimated to be between 0.14 and 0.25 mM (Lehre and Danbolt, 1998). From the transporter density, glutamate transport averaged over a given volume of neuropil can be estimated for any given ambient glutamate value based on Michaelis–Menten kinetics (neglecting exchange, which becomes significant near the equilibrium thermodynamic limit). At steady state, sources and sinks are equal, and the steady-state leak and uptake of glutamate are equal. With ambient [Glu] = 25 nM (Herman and Jahr) and using the lower transporter density estimate of 0.14 mM (Lehre and Danbolt, 1998), the volume-averaged steady-state glutamate leak is predicted to be approximately 2100 molecules μm^{-3} sec^{-1} (but see Cavelier and Attwell, 2005). This tonic leak will cause increased ambient glutamate if transport is reduced, as could occur in a metabolically impaired region of neuropil near a microdialysis probe (Benveniste et al., 1987; Clapp-Lilly et al., 1999; Amina et al., 2003; Bungay et al., 2003; Jaquins-Gerstl and Michael, 2009). We used the diffusion model to describe the spatial profile of [Glu] near a 100 μm radius microdialysis probe with an adjacent damaged region described by a Gaussian gradient of impaired transport (Fig. 4A). Although transporter reversal can occur with severely impaired ion gradients, we neglected this effect, which may underestimate effects of metabolic damage on glutamate measured in the probe. Starting the simulation at time = 0 with no glutamate in the interior of the probe, the glutamate concentration rises with an exponential time constant ~ 8.5 s to a steady state level (data not shown). At steady state, [Glu] inside the probe is elevated relative to the healthy region far from the probe (Fig. 4B_1). With sigma = 0 (i.e. no tissue damage), [Glu] in the probe is equal to the ambient [Glu] in the healthy tissue. With gradients of damage from sigma = 100 to 300 μm, steady-state glutamate levels in the probe range from ~3 to 10 μM (Fig. 4B_1). Decreasing the glutamate diffusion coefficient from its value in buffer, which is higher than in brain (Kullmann et al., 1999), increases the predicted steady state [Glu] measured in the probe (Fig. 4B_2). Increasing or decreasing the leak rate L (Fig. 4B_3) also influences steady state [Glu] predicted in the probe volume.

4. Discussion

Glutamate transporters limit receptor activity on different time scales in the brain by restricting the spread of synaptically released glutamate as well as by maintaining low ambient glutamate concentrations (for reviews, see Danbolt, 2001; Tzingounis and Wadiche, 2007; Vandenberg and Ryan, 2013). The steady-state

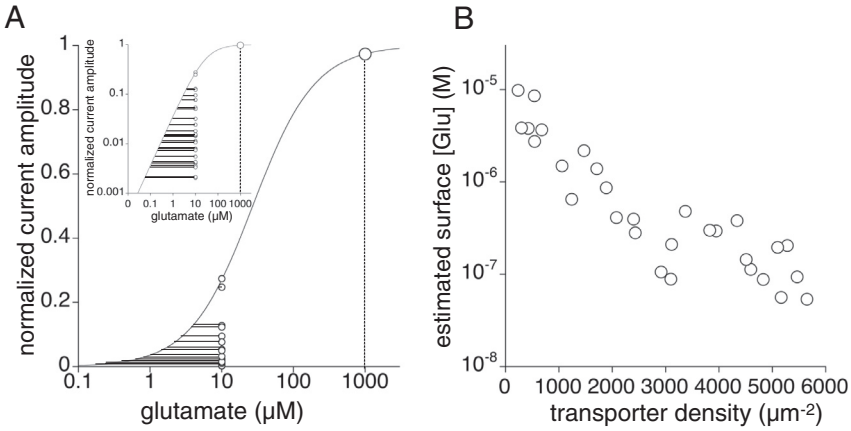

Fig. 3. Surface [Glu] estimates as a function of transporter density. Surface [Glu] estimated from relative amplitude of steady state current amplitude without flow to the 1 mM steady state glutamate current with flow fitted to Michaelis–Menten function ($K_M = 26.8$ μM) (A, semi-log plot; inset, double-log plot) and plotted as a function of transporter density (B) for each oocyte at −60 mV.

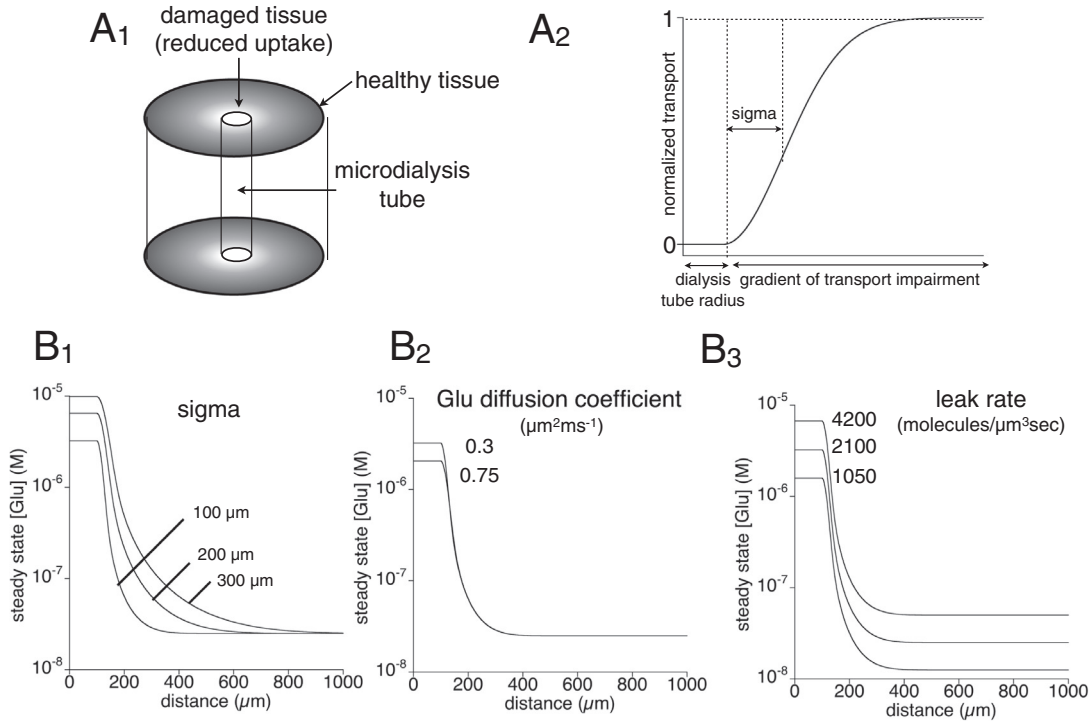

Fig. 4. Diffusion model of transporter contribution in dialysis measurement. (A_1) Cartoon of metabolic damage in Gaussian region surrounding the microdialysis tube. (A_2) Reduced uptake rate described by the Gaussian function in the damaged region. (B) PDE numerical modeling describing the spatial profile of steady-state [Glu] with varying sigma (B_1), diffusion constant (B_2) and leak rate (B_3).

ambient concentration of extracellular glutamate at any point in brain reflects the balance of fluxes through sources and sinks in the neuropil. The data presented here indicate that transporters can establish steep concentration gradients when glutamate is supplied by passive diffusion from a pseudo-infinite source. Although we have used the neuronal transporter EAAT3 in these studies, its equilibrium thermodynamics are indistinguishable from the predominant astroglial transporter EAAT2 (Levy et al., 1998). With EAAT3 transporter densities similar to those reported for EAAT2 in hippocampal astroglial membranes ($\sim 10^4/\mu m^2$; Lehre and Danbolt, 1998) the concentration gradient between a 10 µM source concentration and the cell surface was found to exceed two orders of magnitude. The steepness of the gradient formed would be further increased if diffusion were reduced, as for example in tortuous neuropil (Kullmann et al., 1999). Conversely, reduction of transporter density or activity will reduce the steepness of the gradient and increase [Glu] at the cell surface. Reduced glutamate transport by loss or metabolic impairment is implicated in a broad range of neurodegenerative disorders (Sheldon and Robinson, 2007) including stroke (Rossi et al., 2000), traumatic brain injury (Goodrich et al., 2013), epilepsy (Coulter and Eid, 2012), Huntington's disease (Faideau et al., 2010), ALS (Rothstein, 2009), and Alzheimer's disease (Scimemi et al., 2013).

While a precise knowledge of the concentration of ambient glutamate in various brain regions in normal and neuropathological conditions is desirable, reports of this value in the literature vary widely, with microdialysis approaches consistently providing estimates approximately two orders of magnitude greater than estimates based on electrophysiological measurement of tonic glutamate receptor activity. In the absence of transporter inhibition, ambient [Glu] has been reported as being too low to activate AMPA receptors, even when desensitization is pharmacologically blocked (Le Meur et al., 2007). In contrast, ambient [Glu] has been reported to tonically activate high-affinity NMDA receptors (Sah et al., 1989; Cavelier and Attwell, 2005; Le Meur et al., 2007; Herman and Jahr, 2007). Several patch clamp studies in acute hippocampal slice have provided estimates of ambient [Glu] based on analyses of the tonic NMDA receptor currents in CA1 pyramidal neurons. These have been reported as ~25 nM at 32° (Herman and Jahr, 2007), 27–33 nM at 25° and 77–89 nM at 35° (Cavelier and Attwell, 2005), and 83–87 nM at 25° (Le Meur et al., 2007). These estimates are not likely to be artifactually low due to loss of glutamate from the surface of the slice, because inclusion of 2 µM glutamate in the recording chamber did not alter the level of tonic receptor activity (Herman and Jahr, 2007). The major source of glutamate in these studies was of non-vesicular origin. A range of possible molecular mechanisms may underlie glutamate release, including glutamate-permeable anion channels, the cystine-glutamate exchanger xCT, and passive membrane diffusion (Kimelberg et al., 1990; Baker et al., 2002; Cavelier and Attwell, 2005; for review see Cavelier et al., 2005). Elevation of ambient [Glu] by inhibition of glutamine synthetase suggests that a major contribution of glutamate release is from glia (Cavelier and Attwell, 2005; Le Meur et al., 2007).

The data and the diffusion model presented here suggests that a thin layer of damaged tissue with disrupted glutamate transport could underlie the significant quantitative discrepancy between the ambient glutamate estimates provided by electrophysiological studies in slices and those from microdialysis studies, which generally report ambient [Glu] values in the range $\geqslant 2$ µM (reviewed by Cavelier et al., 2005; Featherstone and Shippy, 2008). Histological analyses of tissue surrounding microdialysis probes provide evidence for a layer of damaged tissue up to hundreds of microns surrounding the probe (Clapp-Lilly et al., 1999; Bungay et al., 2003; Amina et al., 2003; Jaquins-Gerstl and Michael, 2009). Diffusion modeling suggests that disrupted transport in this region could lead to artifactually large concentrations in the probe volume. A critical assumption in our model is that the glutamate leak

source is constant in a volume of metabolically damaged tissue where transport is impaired. The precise spatial changes in metabolic activity in a traumatized or ischemic region of tissue are unknown, but the assumption that the leak is constant is conservative. For example, glutamate release is increased by reversed glutamate transport due to impaired Na/K gradients during metabolic challenge (Rossi et al., 2000). With a spatial distribution of transporter impairment modeled with a Gaussian distribution, sigma values as small as 100 μm lead to significant elevation of predicted probe [Glu] (Fig. 4B_1).

In addition to pharmacological block of glutamate uptake leading to increased activation of AMPA and NMDA receptors (Jabaudon et al., 1999, 2000; Cavelier and Attwell, 2005; Le Meur et al., 2007; Herman and Jahr, 2007), ischemia-induced reversed transport also leads to large increases in extracellular [Glu] and pathological receptor signaling (Rossi et al., 2000). Changes are also predicted by the probe diffusion model probe as a consequence of increases in basal glutamate release (Fig. 4B_3). While the value of extracellular [Glu] in the probe dialysate is predicted to significantly exceed ambient [Glu] in healthy tissue far from the probe, the dialysate concentration is also predicted to change in approximate proportion to changes in glutamate homeostasis in distant tissue (Fig. 4B_3). This behavior of the model is consistent with reported changes in dialysate [Glu] in response to factors including transport block, ischemia, and trauma (Benveniste et al., 1984; Hagberg et al., 1985; Baker et al., 2002; Del Arco et al., 2003; Nyitrai et al., 2006).

Acknowledgements

This work was supported by NIHR15 GM088799 to M.P.K.

The authors thank Anastassios Tzingounis for discussions and preliminary kinetic data on transporter density effects.

References

Baker, D.A., Xi, Z.X., Shen, H., Swanson, C.J., Kalivas, P.W., 2002. The origin and neuronal function of in vivo nonsynaptic glutamate. J. Neurosci. 22 (20), 9134–9141.

Barry, P.H., Diamond, J.M., 1984. Effects of unstirred layers on membrane phenomena. Physiol. Rev. 64, 763–872.

Benveniste, H., Drejer, J., Schousboe, A., Diemer, N.H., 1984. Elevation of the extracellular concentrations of glutamate and aspartate in rat hippocampus during transient cerebral ischemia monitored by intracerebral microdialysis. J. Neurochem. 43 (5), 1369–1374.

Benveniste, H., Drejer, J., Schousboe, A., Diemer, N.H., 1987. Regional cerebral glucose phosphorylation and blood flow after insertion of a microdialysis fiber through the dorsal hippocampus in the rat. J. Neurochem. 49 (3), 729–734.

Bungay, P.M., Newton-Vinson, P., Isele, W., Garris, P.A., Justice, J.B., 2003. Microdialysis of dopamine interpreted with quantitative model incorporating probe implantation trauma. J. Neurochem. 86 (4), 932–946.

Cavelier, P., Hamann, M., Rossi, D., Mobbs, P., Attwell, D., 2005. Tonic excitation and inhibition of neurons: ambient transmitter sources and computational consequences. Prog. Biophys. Mol. Biol. 87 (1), 3–16.

Cavelier, P., Attwell, D., 2005. Tonic release of glutamate by a DIDS-sensitive mechanism in rat hippocampal slices. J. Physiol. (Lond.) 564, 397–410.

Clapp-Lilly, K.L., Roberts, R.C., Duffy, L.K., Irons, K.P., Hu, Y., Drew, K.L., 1999. An ultrastructural analysis of tissue surrounding a microdialysis probe. J. Neurosci. Methods 90 (2), 129–142.

Coulter, D.A., Eid, T., 2012. Astrocytic regulation of glutamate homeostasis in epilepsy. Glia 60, 1215–1226.

Danbolt, N.C., 2001. Glutamate uptake. Prog. Neurobiol. 65 (1), 1–105.

Del Arco, A., Segovia, G., Fuxe, K., Mora, F., 2003. Changes in dialysate concentrations of glutamate and GABA in the brain: an index of volume transmission mediated actions? J. Neurochem. 85 (1), 23–33.

Faideau, M., Kim, J., Cormier, K., Gilmore, R., Welch, M., Auregan, G., Dufour, N., Guillermier, M., Brouillet, E., Hantraye, P., et al., 2010. In vivo expression of polyglutamine-expanded huntingtin by mouse striatal astrocytes impairs glutamate transport: a correlation with Huntington's disease subjects. Hum. Mol. Genet. 19, 3053–3067.

Featherstone, D.E., Shippy, S.A., 2008. Regulation of synaptic transmission by ambient extracellular glutamate. Neuroscientist 14 (2), 171–181.

Goodrich, G.S., Kabakov, A.Y., Hameed, M.Q., Dhamne, S.C., Rosenberg, P.A., Rotenberg, A., 2013. Ceftriaxone treatment after traumatic brain injury restores expression of the glutamate transporter, GLT-1, reduces regional gliosis, and reduces post-traumatic seizures in the rat. J. Neurotrauma 30, 1434–1441.

Hagberg, H., Lehmann, A., Sandberg, M., Nyström, B., Jacobson, I., Hamberger, A., 1985. Ischemia-induced shift of inhibitory and excitatory amino acids from intra- to extracellular compartments. J. Cereb. Blood Flow Metab. 5 (3), 413–419.

Herman, M.A., Jahr, C.E., 2007. Extracellular glutamate concentration in hippocampal slice. J. Neurosci. 27 (36), 9736–9741.

Jabaudon, D., Shimamoto, K., Yasuda-Kamatani, Y., Scanziani, M., Gähwiler, B.H., Gerber, U., 1999. Inhibition of uptake unmasks rapid extracellular turnover of glutamate of nonvesicular origin. Proc. Natl. Acad. Sci. USA 96, 8733–8738.

Jabaudon, D., Scanziani, M., Gähwiler, B.H., Gerber, U., 2000. Acute decrease in net glutamate uptake during energy deprivation. Proc. Natl. Acad. Sci. USA 97 (10), 5610–5615.

Jaquins-Gerstl, A., Michael, A.C., 2009. Comparison of the brain penetration injury associated with microdialysis and voltammetry. J. Neurosci. Methods 183 (2), 127–135.

Khan, Amina S., Michael, Adrian C., 2003. Invasive consequences of using micro-electrodes and microdialysis probes in the brain. Trends Anal. Chem. 22 (8), 503–508.

Kimelberg, H.K., Goderie, S.K., Higman, S., Pang, S., Waniewski, R.A., 1990. Swelling-induced release of glutamate, aspartate, and taurine from astrocyte cultures. J. Neurosci. 10, 1583–1591.

Kullmann, D.M., Min, M.Y., Asztély, F., Rusakov, D.A., 1999. Extracellular glutamate diffusion determines the occupancy of glutamate receptors at CA1 synapses in the hippocampus. Philos. Trans. R. Soc. London, B Biol. Sci. 354, 395–402.

Le Meur, K., Galante, M., Angulo, M.C., Audinat, E., 2007. Tonic activation of NMDA receptors by ambient glutamate of non-synaptic origin in the rat hippocampus. J. Physiol. 580 (Pt. 2), 373–383.

Lehre, K.P., Danbolt, N.C., 1998. The number of glutamate transporter subtype molecules at glutamatergic synapses: chemical and stereological quantification in young adult rat brain. J. Neurosci. 18 (21), 8751–8757.

Lerma, J., Herranz, A.S., Herreras, O., Abraira, V., Martín del Río, R., 1986. In vivo determination of extracellular concentration of amino acids in the rat hippocampus. A method based on brain dialysis and computerized analysis. Brain Res. 384 (1), 145–155.

Levy, L.M., Warr, O., Attwell, D., 1998. Stoichiometry of the glial glutamate transporter GLT-1 expressed inducibly in a Chinese hamster ovary cell line selected for low endogenous Na^+-dependent glutamate uptake. J. Neurosci. 18, 9620–9628.

Nyitrai, G., Kékesi, K.A., Juhász, G., 2006. Extracellular level of GABA and Glu: in vivo microdialysis-HPLC measurements. Curr. Top. Med. Chem. 6 (10), 935–940.

Rossi, D.J., Oshima, T., Attwell, D., 2000. Glutamate release in severe brain ischaemia is mainly by reversed uptake. Nature 403 (6767), 316–321.

Rothstein, J.D., 2009. Current hypotheses for the underlying biology of amyotrophic lateral sclerosis. Ann. Neurol. 65 (Suppl 1), S3–9.

Sah, P., Hestrin, S., Nicoll, R.A., 1989. Tonic activation of NMDA receptors by ambient glutamate enhances excitability of neurons. Science 246 (4931), 815–818.

Scimemi, A., Meabon, J.S., Woltjer, R.L., Sullivan, J.M., Diamond, J.S., Cook, D.G., 2013. Amyloid-β1-42 slows clearance of synaptically released glutamate by mislocalizing astrocytic GLT-1. J. Neurosci. 33, 5312–5318.

Sheldon, A.L., Robinson, M.B., 2007. The role of glutamate transporters in neurodegenerative diseases and potential opportunities for intervention. Neurochem. Int. 51, 333–355.

Supplisson, S., Bergman, C., 1997. Control of NMDA receptor activation by a glycine transporter co-expressed in Xenopus oocytes. J. Neurosci. 17 (12), 4580–4590.

Tzingounis, A., Wadiche, J., 2007. Glutamate transporters: confining runaway excitation by shaping synaptic transmission. Nat. Rev. Neurosci. 8 (12), 935–947.

Vandenberg, R.J., Ryan, R.M., 2013. Mechanisms of glutamate transport. Physiol. Rev. 93, 1621–1657.

Wadiche, J.I., Arriza, J.L., Amara, S.G., Kavanaugh, M.P., 1995. Kinetics of a human glutamate transporter. Neuron 14, 1019–1027.

Zerangue, N., Kavanaugh, M.P., 1996. Flux coupling in a neuronal glutamate transporter. Nature 383, 634–637.

Zorumski, C.F., Mennerick, S., Que, J., 1996. Modulation of excitatory synaptic transmission by low concentrations of glutamate in cultured rat hippocampal neurons. J. Physiol. (Lond.) 494 (Pt 2), 465–477.

Zuo, Z., Fang, H., 2005. Glutamate transporter type 3 attenuates the activation of N-methyl-D-aspartate receptors co-expressed in Xenopus oocytes. J. Exp. Biol. 208 (Pt 11), 2063–2070.